

# Characterization and composition evolution of multiple-phase nanoscaled ceramic powders produced by laser ablation

Shih-Chin Lin<sup>a</sup>, San-Yuan Chen<sup>a,\*</sup>, Syh-Yuh Cheng<sup>b</sup>

<sup>a</sup>Material Science and Engineering, National Chiao Tung University, Hsinchu 300 Taiwan, Republic of China

<sup>b</sup>Materials Research Laboratories, Industrial Technology Research Institute, Taiwan, Republic of China

## Abstract

Nanosized ceramic powder was prepared by laser ablation under different atmospheres using a ceramic target composed of ZrO<sub>2</sub>, TiO<sub>2</sub>, ZnO and Al<sub>2</sub>O<sub>3</sub>. Physical characteristics and microstructure of nanoparticles, including particle morphology, phase transformation, powder compositions and far-infrared emissivity, have been investigated. The laser-ablated nanoparticles exhibit two kinds of particle size distribution with 7–15 (70–90%) and 40–100 nm (10–30%). Nanoparticles synthesized at lower laser fluences show poor crystallinity but rich Zn composition. While increasing laser fluence, better crystalline nanoparticles with rich Zr composition were obtained. It was found that both composition and morphology of nanoparticles change with laser fluence. The average far-infrared emissivity of the nanoparticles varies with crystallinity of nanoparticles.

© 2004 Elsevier B.V. All rights reserved.

PACS: 73.61.Tm; 81.15.Fg; 81.40.-z

Keywords: Nanoparticle; Laser ablation; Multiphase; Phase separation; Far-infrared emission

## 1. Introduction

During the past few years, various methods, including physical and chemical vapor condensation [1,2], chemical routes [3,4] and laser ablation [5], have been developed to prepare inorganic nanoparticles. Many methods have been developed to prepare inorganic nanoparticles. [4] Chemical route usually use metal-organic compounds as precursors to synthesize nanoparticles through hydrolysis, condensation, catalysis and pyrolysis, etc. On the other hand, evaporation–condensation is mainly the dominant process in physical route. Laser ablation is the main physical process for nanoparticle. High pulse laser energy impacts material surface to form nanoparticles. Although there is still a reaction mechanism of laser–surface interaction needed to be disclosed in laser ablation, it is a useful method for nanoparticle synthesis. For complex or multi-

phase oxide, laser ablation gives convenient and effective technical solution. Composition and phase of ablated particle are easily adjustable through composition/phase modification of target.

It was reported that the far-infrared emission of the materials can be improved when transitional element oxide was added [6,7]. Therefore, in this work, ceramic target composed of complex oxides, including Al<sub>2</sub>O<sub>3</sub>, ZnO, TiO<sub>2</sub> and ZrO<sub>2</sub>, will be used for the study. Effect of processing conditions including laser power, atmosphere and flow rate of carrier gas on composition, particle size distribution and phase evolution of laser-ablated nanoparticles will be investigated. In addition, the far-infrared emissivity characteristic of nanoparticles as functions of laser powder and atmosphere are also presented.

## 2. Experimental

The ceramic targets for the laser ablation were prepared following the conventional ceramic process.

\* Corresponding author.

E-mail address: [syichen@cc.nctu.edu.tw](mailto:syichen@cc.nctu.edu.tw) (S.-Y. Chen).

ZrO<sub>2</sub>:TiO<sub>2</sub>:ZnO:Al<sub>2</sub>O<sub>3</sub> with the molar ratio of 1:1: 2:2 were mixed and then compressed into a 30-mm-diameter green compact. Excimer laser (248 nm) power was varied to study the ablation efficiency. The laser fluences of 0.34, 1 and 4 J/cm<sup>2</sup> were used for the generation of nanoparticles in this work. Three carrier gases, including air, oxygen and nitrogen, were used with ambient atmospheres remained around 1 atm.

A transmission electron microscope (TEM) was used for determining composition and morphology of nanoparticles. The atomic ratio of element Zr, Ti, Zn and Al was semiquantitatively determined through EDS analysis. Crystal phase was identified through X-ray diffraction and selected area electron diffraction pattern. Surface image and mapping analysis were obtained from field emission scanning electron microscope (FE-SEM). Far-infrared emissivity characterization of nanoparticles was measured by using infrared spectrophotometer with black body furnace as a reference beam source.

### 3. Results and discussion

#### 3.1. Microstructure evolution of ablated target

The XRD patterns in Fig. 1a illustrate that only ZrTiO<sub>4</sub>, ZnAl<sub>2</sub>O<sub>4</sub> and residual ZrO<sub>2</sub> were detected from laser-ablated target. It reveals that some interreaction occurs in the target during laser ablation and causes different phase evolutions from the original ceramic powder. The surface element mapping of laser-ablated target was further examined and shown in Fig. 2 which discloses that the prominent area contains rich Zr, but the composition in the concave area shows rich Zn. This indicates that Zr-rich area was subjected to a lower ablation rate, but a higher ablation rate occurs at Zn-rich area under the same laser fluence of 0.34 J/cm<sup>2</sup>. In other words, Zn is more easily laser-ablated out of the target

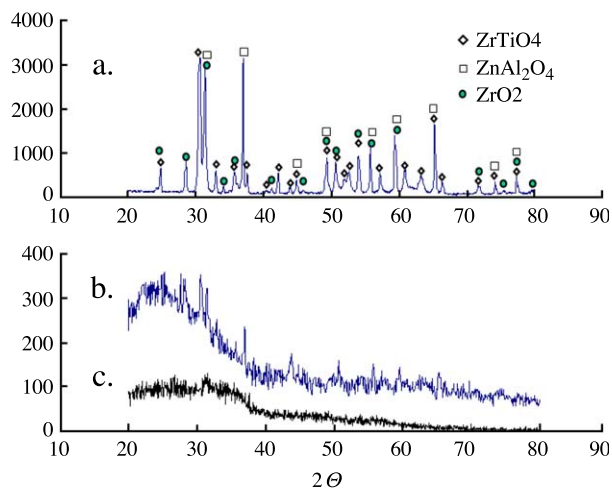


Fig. 1. XRD patterns of (a) laser-ablated target and nanoparticles produced by (b) 4 and (c) 0.34 J/cm<sup>2</sup> laser fluence in air atmosphere.

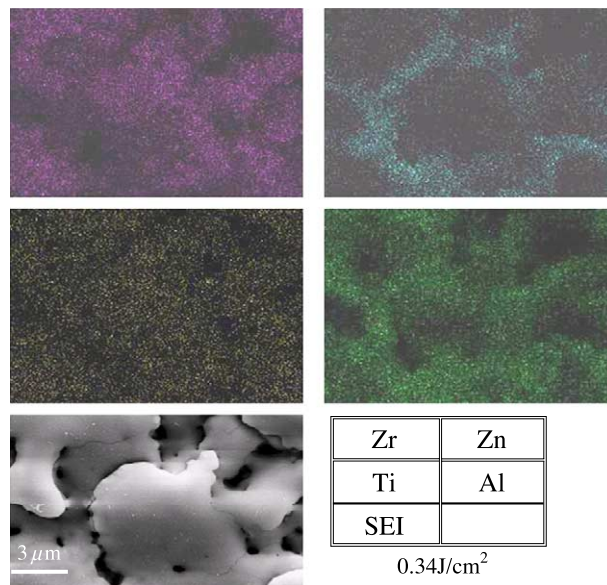


Fig. 2. Surface mapping of laser-ablated target under 0.34 J/cm<sup>2</sup> laser fluence in air atmosphere.

compared to Zr element. In addition, it was found that the element distribution of Al is similar to Zn element in the target. However, Ti element could be found at the whole area. This observation demonstrates that phase separation and inhomogeneous composition often occurred when multiphase or complex oxides are used.

#### 3.2. Morphology of ablated nanoparticles

Fig. 1b and c illustrates that the nanoparticles generated by 4 and 0.34 J/cm<sup>2</sup> laser fluences show poor crystallite and amorphous-like structure, respectively. Two kinds of particle size distribution with fine nanoparticles of 5–20 nm (70–90%) and large spherical nanoparticles of 40–100 nm

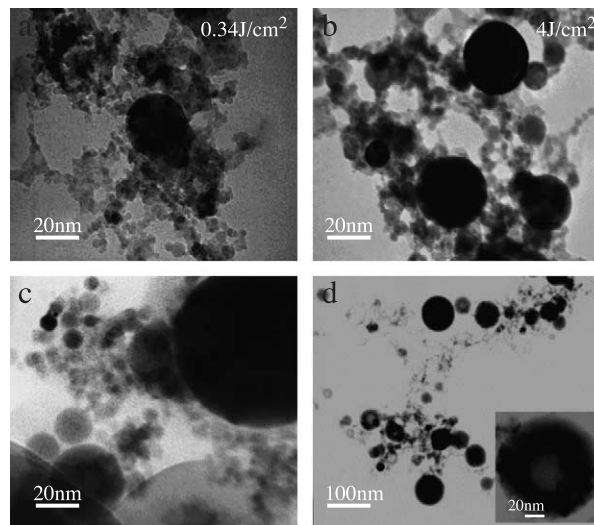


Fig. 3. TEM photographs of nanoparticles produced by (a) 0.34 and (b) 4 J/cm<sup>2</sup> laser fluence in air atmosphere; and (c) in nitrogen atmosphere and (d) in oxygen atmosphere at 4 J/cm<sup>2</sup> laser fluence.

(10–30%) were obtained in both cases, as shown in Fig. 3a and b. It was also observed that as a stronger laser fluence was applied, the number of large spherical particles is increased. The average particle size of 8.2, 10.7 and 11.6 nm was obtained under 0.34, 1 and 4 J/cm<sup>2</sup> of laser fluence, respectively. Fig. 4 illustrates the influence of laser power on the phase crystallization of nanoparticles. Generally, the phase crystallization increases with a stronger fluence. The electron diffraction pattern shows better crystalline particle for high laser power (4 J/cm<sup>2</sup>), but lower laser power gives an amorphous-like particle. The higher laser power digs out larger particle with liquid phase on its surface. Good crystallization is also observed for these large particles. When a lower laser power is applied, only gas-like particles are excited and will be consolidated into amorphous phase because of the quench effect of flow gas or atmosphere.

As the nanoparticles were synthesized in nitrogen atmospheres, Fig. 3c presents a broader particle distribution as compared to that synthesized in air atmospheres. Furthermore, it was noted that, in oxygen atmospheres, some hollow nanoparticles, as shown in Fig. 3d, appear in large spherical nanoparticles of 40–100 nm that were generated at a higher laser power (4 J/cm<sup>2</sup>). Larger spherical nanoparticles were richer in Zr element and poorer in Zn element as compared to fine nanoparticles of 5–20 nm that never showed a hollow structure. It was believed that vaporization of Zn atom and the cooling effect are responsible for the generation of hollow nanoparticles.

### 3.3. Phase separation of ablated nanoparticles

The composition of the generated nanoparticles was examined by TEM and EDS analysis based on a normalized molar ratio of atoms with Zr+Ti+Zn+Al=100%. Fig. 5 shows the relative content of different elements for the three types of nanoparticles under different fluences in air atmosphere. In other words, these three types of nanoparticles can be generated under each laser fluence, but they have different composition distribution. It was found that, for finer nanoparticles (5–20 nm), with an increase of laser fluence, Zn content decreases but Zr content increases. In addition, both Al and Ti contents present similar trend to Zr but show more irregularity. However, in the case of large spherical nanoparticles (40–100 nm), the Zn content was

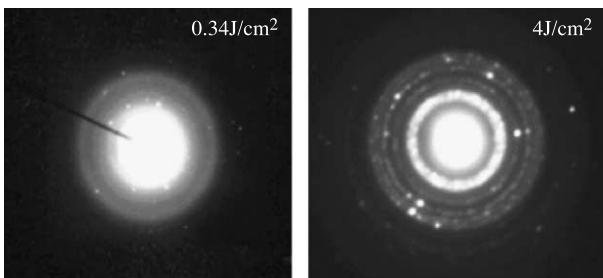


Fig. 4. Dependence of phase crystallization of laser-ablated nanoparticles on laser fluence.

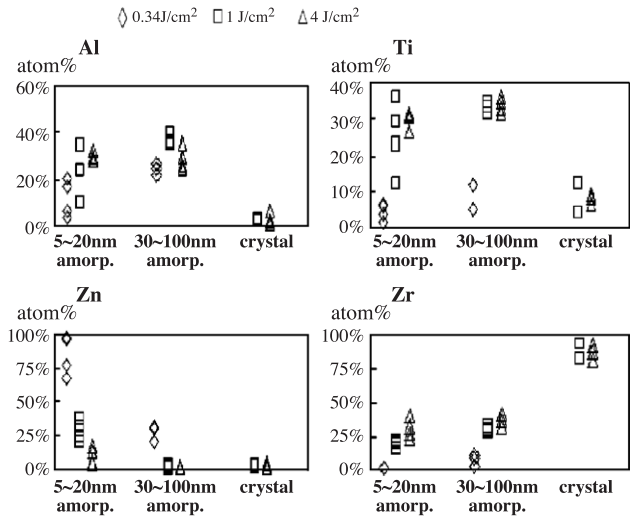


Fig. 5. Relative element ratio of three types of nanoparticles under different fluences in air atmosphere.

apparently decreased, but the content in the other elements is increased with increasing laser fluence. It was believed that as the fine nanoparticles were condensed from vapor phase, more Zn content would be easily trapped because Zn element was more easily evaporated into gas phase than the others. In contrast, as the larger crystalline particles were formed, the EDS shows that it was primarily composed of Zr (more than 70%) with little Zn. It was believed that the element distribution of the generated nanoparticles was related to kinetics and thermodynamics of vapor composition and atom density during laser ablation. Therefore, up to now, it is very difficult to clearly explain it for the present multiple composition system.

### 3.4. Far-infrared ray emissivity characterization

The far-infrared emissivity characterization of nanoparticles was investigated with black body furnace as a reference of 1. It was found that the average emissivity of the collected particles was as a function of particle size and phase crystallization. Higher laser power of 4 J/cm<sup>2</sup> gives a larger average emission (91%) compared to that (79%) of nanoparticles synthesized at a low laser power (0.34 J/cm<sup>2</sup>). Although the former obtains large spherical particles, it was believed that both composition control and good crystallization dominate the main contribution on the far-infrared emissivity. Further results which will be connected to more detailed analysis will be reported later.

## 4. Conclusion

Although the ablated target was prepared from ceramic powders of ZrO<sub>2</sub>, TiO<sub>2</sub>, ZnO and Al<sub>2</sub>O<sub>3</sub>, the generated nanoparticles exhibit different compositions after laser ablation in different atmospheres. It was found that phase separation and inhomogeneous composition often occur for

this multiple-composition system. Depending on laser power and atmosphere, nanoparticles with different composition are obtained. Higher laser power creates larger particle with good crystallization and stronger far-infrared emissivity, while lower one gives fine nanoparticles with amorphous-like structure and weak far-infrared emissivity.

### Acknowledgements

The authors gratefully acknowledge the financial support by Ministry of Economic Affairs of the Republic of China through 92-EC-17-A-08-R7-0312 Contract.

### References

- [1] M. Choi, *J. Nanopart. Res.* 3 (2001) 201.
- [2] Z. Paszti, G. Peto, Z.E. Horvath, A. Karacs, *Appl. Surf. Sci.* 168 (2000) 114.
- [3] K. Landfester, *Adv. Mater.* 13 (2001) 765.
- [4] Y.C. Kang, S.B. Park, Y.W. Kang, *Nanostruct. Mater.* 5 (1995) 771.
- [5] T. Sasaki, S. Terauchi, N. Koshizaki, H. Umehara, *Appl. Surf. Sci.* 127–129 (1998) 398.
- [6] H. Takashima, *Yogyo kyokai-Shi* 89 (1981) 655.
- [7] H. Takashima, K. Matsubara, Y. Nishimura, E. Kato, *Yogyo kyokai-Shi* 90 (1982) 373.